Traffic 2007; **8:** 1829–1840
Blackwell Munksgaard

doi: 10.1111/j.1600-0854.2007.00658.x

Dominant-Negative Behavior of Mammalian Vps35 in Yeast Requires a Conserved PRLYL Motif Involved in Retromer Assembly

Xiang Zhao[1], Steven Nothwehr[2], Roberto Lara-Lemus[1], Bao-yan Zhang[3], Harald Peter[4] and Peter Arvan[1,*]

[1]Division of Metabolism, Endocrinology & Diabetes, University of Michigan, 5560 MSRB2, 1150 W. Medical Center Drive, Ann Arbor, MI 48109, USA
[2]Division of Biological Sciences, University of Missouri, 401 Tucker Hall, Columbia, MO 65211, USA
[3]Ophthalmology and Visual Sciences, University of Wisconsin Medical School, 406 Science Drive, Madison, WI 53711, USA
[4]Institute of Technical Biochemistry, University of Stuttgart, Allmandring 31, D-70569 Stuttgart, Germany
**Corresponding author: Peter Arvan, parvan@umich.edu*

The retromer protein complex assists in recycling selected integral membrane proteins from endosomes to the *trans* Golgi network. One protein subcomplex (Vps35p, Vps26p and Vps29p) combines with a second (Vps17p and Vps5p) to form a coat involved in sorting and budding of endosomal vesicles. Yeast Vps35p (yVps35) exhibits similarity to human Vps35 (hVps35), especially in a completely conserved PRLYL motif contained within an amino-terminal domain. Companion studies indicate that an $R_{98}W$ mutation in yVps35 causes defective retromer assembly in *Saccharomyces cerevisiae*. Herein, we find that the expression of hVps35 in yeast confers dominant-negative vacuolar proenzyme secretion and defective secretory proprotein processing. The mutant phenotype appears to be driven by hVps35 competing with endogenous yVps35, becoming incorporated into defective retromer complexes and causing proteasomal degradation of endogenous Vps26 and Vps29. Increased expression of yVps35 displaces some hVps35 to a 100 000 × *g* supernatant and suppresses the dominant-negative phenotype. Remarkably, mutation of the conserved $R_{107}W$ of hVps35 displaces some of the protein to the 100 000 × *g* supernatant, slows protein turnover and restores stability of Vps26p and Vps29p and completely abrogates dominant-negative trafficking behavior. We show that hVps35 coprecipitates Vps26, whereas the $R_{107}W$ mutant does not. In pancreatic beta cells, the $R_{107}W$ mutant shifts hVps35 from peripheral endosomes to a juxtanuclear compartment, affecting both mannose phosphate receptors and insulin. These data underscore importance of the Vps35 PRLYL motif in retromer subcomplex interactions and function.

Key words: coat protein, endosome, protein sorting, protein trafficking, retromer, secretory pathway

Received 4 April 2007, revised and accepted for publication 20 September 2007, published online 17 October 2007

It has previously been shown that upon expression of an insulin-containing fusion protein in *Saccharomyces cerevisiae*, molecules that fail to undergo Kex2-mediated endoproteolysis are rapidly secreted, whereas the processed insulin fraction is transported to the vacuole (1). A genetic screen identified six single gene disruptions allowing enhanced immunoreactive insulin secretion because of defective Kex2-mediated endoproteolytic processing; of these, *vps35* showed the strongest phenotype (1). *VPS35* encodes a subunit of retromer, a coat protein complex engaged in the retrieval of recycling membrane proteins from endosomes to the *trans* Golgi network (2). Protein recycling is essential for protein sorting in the vacuolar/lysosomal biogenesis pathway as well as for lumenal protein processing in both secretory and endosomal systems (3). Moreover, retromer function is essential for the development and viability of mammalian organisms (4).

The core of the retromer protein complex involves a large protein subcomplex comprised of Vps35, Vps29 and Vps26 (5) along with a smaller subcomplex comprised of Vps17 and Vps5 (6). With potential contributions from ancillary proteins, these two subcomplexes assemble into a multimeric membrane coat. Of the members of the retromer complex, yeast Vps35 has been shown to directly bind to the structural information encoded in the cytosolic domains of recycling integral membrane proteins (7,8), which could help to sequester these proteins into endosomal-derived membrane recycling intermediates (5). Vps26 binds to Vps35 and has been implicated as a potential molecular bridge between the two protein subcomplexes (9).

The ease of yeast genetics has facilitated advances in understanding eukaryotic protein sorting and recycling in the secretory/endosomal pathways. The function of the mammalian retromer complex is similar to that found in simpler eukaryotes (10,11), and its subunits exhibit structural conservation with those of yeast (12) and plants (13). The activity of mammalian–yeast chimeras of retromer proteins (9) underscores the commonality of their function through retention of conserved domains. With respect to lysosomal biogenesis, analogous to its function in yeast, human Vps35 (hVps35) actively engages and assists in the recycling of the cation-independent mannose 6-phosphate receptor (CI-MPR) (8,14). In subcomplex assembly, two-hybrid analyses and pull-down experiments suggest that hVps26 and hVps29 bind independently to an N-terminal and C-terminal region, respectively, of hVps35 (15,16).

Regarding the N-terminal region, recent studies suggest that the $PRLYL_{101}$ motif in yeast Vps35 (yVps35) is likely to be an important site for protein interaction with Vps26, requiring the R_{98} residue of yVps35 (17).

In the present study of yeast cells, we have tried to examine the ability of hVps35 (which shares a highly conserved amino-terminal domain including 100% identity in the $PRLYL_{110}$ motif) to interact with the yeast retromer complex. We now establish this conserved amino-terminal domain as responsible for hVps35 behaving as a dominant negative in yeast cells, which is entirely dependent upon the presence of R_{107} (the functional equivalent of R_{98} in yVps35), and the binding activity of this residue for Vps26.

Results

The conserved amino-terminal domain of yVps35 and hVps35

Potential dominant-negative alleles of yeast *VPS35* were prepared by random mutagenesis, subcloned into a low-copy centromeric plasmid, transformants screened for increased carboxypeptidase Y (CPY) secretion and dominant-negative constructs rescued and sequenced (17). Notable amongst these was the high percentage of mutants that possessed alteration at the R_{98} residue contained within a conserved motif between yVps35 and hVps35 such that R_{98} of yVps35 corresponds to residue R_{107} in hVps35 (Figure 1A). Indeed, a single yVps35R_{98}W mutant functions as a dominant negative in vacuolar protein sorting, indicating that at least one yVps35 partner protein interaction is lost by this mutation (17).

A chimeric protein (nhcy1: N-human, C-yeast) containing the N-terminal region of hVps35 up to residue 263 fused in frame to residues 245–944 of yVps35 was prepared to examine whether this hVps35 region (including the nearly identical A_{83}–G_{106} region) was functional in yeast and whether subsequent introduction of the R_{107}W mutation would confer a similar dominant-negative vacuolar protein sorting phenotype. Indeed, in a *vps35*Δ background, nhcy1 expression could complement partially with virtually all activity lost in the presence of the R_{107}W mutation (Figure 1B). This was confirmed quantitatively by CPY immunoprecipitation after pulse-chase analysis (Figure 1C). In a wild-type strain background, dominant-negative *vps* behavior of nhcy1 was augmented by introduction of the R_{107}W mutation (Figure 1D) and confirmed by quantitative CPY immunoprecipitation (Figure 1E). These data argue strongly that R_{98} of yVps35, and the homologous R_{107} of hVps35, is likely to be an important conserved residue for interaction within the yeast retromer complex.

Dominant-negative action of hVps35 in yeast cells

In addition to untagged hVps35, two versions of hVps35 were prepared that were epitope tagged on the amino or carboxyl terminus, respectively. Despite being driven by the strong *TDH3* promoter, none of these versions could complement a *vps35*Δ mutant (Figure 2A). However, HA-hVps35, C-terminal myc-tagged human Vps35 (hVps35-myc) and untagged hVps35, each exhibited comparable perturbation of vacuolar protein sorting relative to wild-type yeast transformed with an empty vector (Figure 2B). By pulse-chase analysis, expression of either hVps35-myc or HA-hVps35 induced significant secretion of the newly synthesized P2 (post Golgi) form of CPY, accompanied by a dramatic reduction in the intracellular appearance of the mature vacuolar CPY (Figure 2C). For convenience, most of the further studies employed hVps35-myc. Expression of *TDH3*-hVps35-myc also interfered with proalpha factor processing (Figure 3). Thus, hVps35 exhibited dominant-negative behavior on protein trafficking within the secretory/endosomal system.

If hVps35 competes with yVps35 for one or more retromer-binding partners, then such dominant-negative behavior might be expected to be suppressed under conditions where yVps35 protein is overexpressed. As predicted, expression of *VPS35* on a high-copy plasmid resulted in decreased CPY secretion from strains bearing hVps35-myc (Figure 4A).

Consistent with the notion that hVps35 engages in protein interaction with endogenous yeast retromer, we found that hVps35-myc was essentially, quantitatively pelleted with membranes after 1 h at 100 000 × ***g*** (Figure 4B). When the expression of yVps35 was increased, a modestly increased fraction of hVps35-myc could be recovered in the supernatant, suggesting some degree of displacement of hVps35-myc by yVps35. These data strongly suggest that the dominant-negative behavior of hVps35 represents competition with yVps35 for binding with partners in the retromer endosomal membrane coat.

R_{107} is required for the dominant-negative activity of hVps35 in yeast cells

To test the role of R_{107} within the conserved PRLYL motif in the association of hVps35 with the yeast retromer, we created the hVps35R_{107}W-myc mutant and examined its effect on CPY secretion and proalpha factor processing. As shown in Figure 5A, the hVps35R_{107}W mutant is indeed expressed as a myc-Western blottable protein (of approximately 75 kDa) in yeast cell lysates. However, while hVps35 exhibited a clear dominant-negative vacuolar protein sorting defect, hVps35R_{107}W was without effect on CPY secretion (Figure 5B; with comparable effects observed in pulse-chase experiments, not shown). Similarly, the proalpha factor processing defect of hVps35 was abrogated by the presence of the R_{107}W mutation (Figure 5C).

We examined the effect of the R_{107}W mutation on the relative stability and sedimentation of hVps35 in yeast cells. As shown in Figure 6A, newly synthesized (metabolically

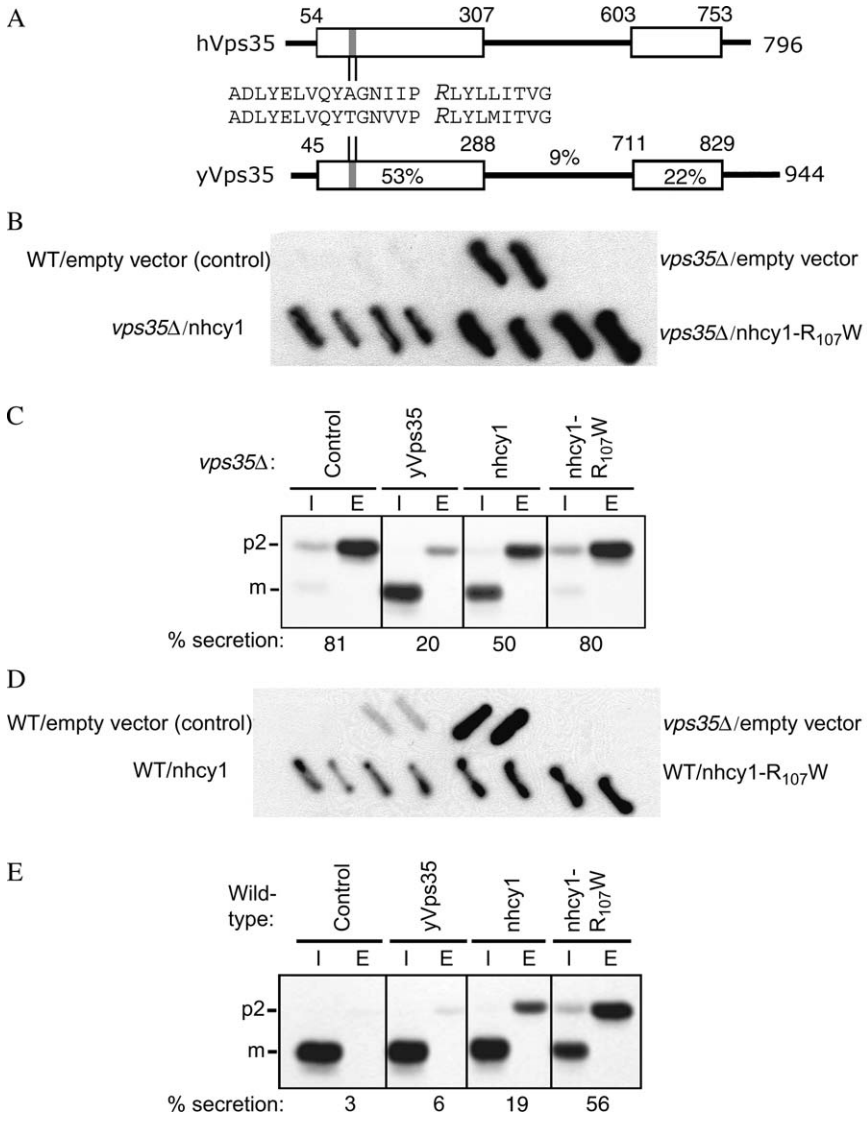

Figure 1: Mutation of the conserved R_{107} residue induces a dominant-negative phenotype in the context of a chimera of hVps35–yVps35. A) Within a conserved domain extending to residue 288 of yVps35, a sequence of near identity surrounds yVps35-R_{98}, corresponding to hVps35-R_{107} (enlarged font). The 'nhcy1' chimera was constructed to contain the N-terminal 263 residues of hVps35 linked to C-terminal residues 245–944 of yVps35. Panels B–E each employ low-copy YCp plasmids with expression driven by the *TDH3* promoter. B) Wild-type (WT) (W303) and *vps35*Δ mutant strains are shown in duplicate above, while nhcy1 (in quadruplicate) exhibits partial complementation of vacuolar protein sorting in a *vps35*Δ background. The R_{107}W mutant of nhcy1 exhibits no complementation. C) *vps35*Δ mutant cells transformed with empty vector (control) or plasmids encoding yVps35, nhcy1 or nhcy1-R_{107}W were pulse labeled for 10 min with ^{35}S-amino acids and chased for 45 min before immunoprecipitation of CPY from intracellular (I) and extracellular (E) fractions. Quantification of these data is summarized beneath the panel. D) Wild-type control (W303) and *vps35*Δ mutant strains are shown above, while the nhcy1 mutant (in quadruplicate) produces a milder dominant-negative phenotype than does the nhcy1-R_{107}W mutant. Not shown in panels B + D: expression of yVps35 in *vps35*Δ cells resulted in CPY secretion comparable to controls. E) Wild-type SNY36-9A cells transformed with empty vector (control) or plasmids encoding expression of yVps35, nhcy1 or nhcy1-R_{107}W were analyzed as in panel C with quantification of the data shown below. 'p2' form = uncleaved Golgi-modified precursor; 'm' form = mature vacuolar species.

labeled) hVps35-myc exhibited a slightly higher turnover than did hVps35R_{107}W-myc (discussed further below). Significantly, although a high degree of sedimentation was observed after 1 h at 100 000 × ***g***, a modestly increased fraction of hVps35R_{107}W-myc could be recovered in the supernatant compared with that seen for hVps35-myc (Figure 6B), indicating diminished membrane association for the R_{107}W mutant. The latter results suggest that hVps35, by virtue of R_{107}, participates in a defective membrane-bound yeast retromer complex.

A recent study suggests that the PRLYL$_{101}$ motif of yVps35 is engaged with yVps26 (17). To determine if R_{107} of hVps35 similarly engages yVps26, coimmunoprecipitation

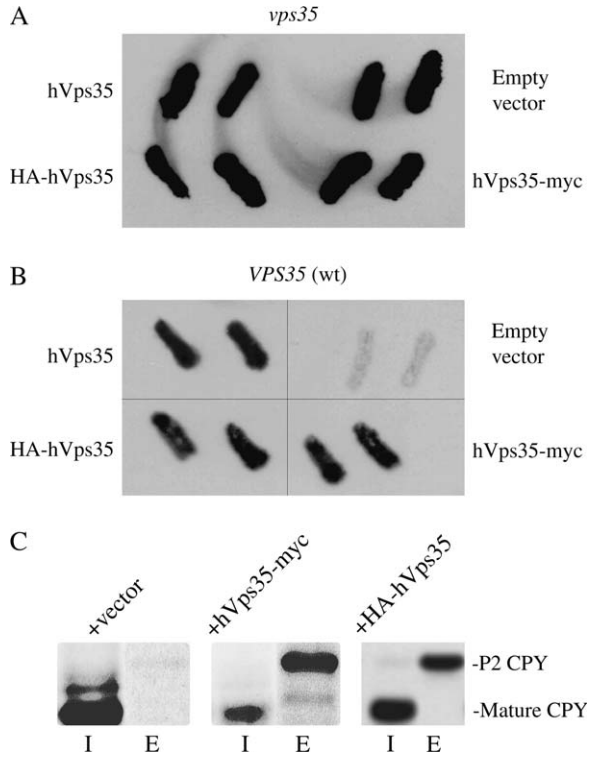

Figure 2: Untagged or tagged hVps35 induces a dominant-negative vacuolar sorting phenotype in yeast. Panels A–C each employ low-copy YCp plasmids with expression driven by the *TDH3* promoter. A) Unlike wild-type yVps35 (not shown), none of the constructs shown can complement vacuolar protein sorting in a *vps35*Δ mutant. B) Transformation of wild-type (wt) cells to express each of the constructs shown induces CPY secretion beyond that observed for cells transformed with an empty vector. C) Cells expressing C-terminally myc-tagged or N-terminally HA-tagged hVps35 secrete the post Golgi (P2) form of CPY to the extracellular medium (E) with decreased mature CPY retained intracellularly (I).

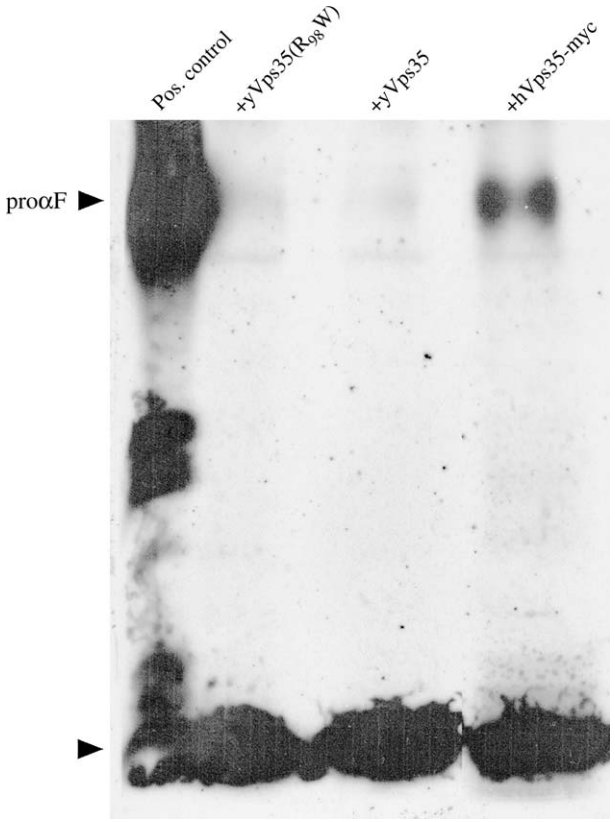

Figure 3: Proalpha factor (proαF) secretion from cells expressing hVps35. Wild-type yeast bearing plasmids expressing the indicated proteins (yVps35 constructs expressed from multi-copy Yep plasmids driven by the *VPS35* promoter; hVps35myc from a YCp plasmid with expression driven by the *TDH3* promoter) were metabolically labeled with ^{35}S-amino acids for 50 min as described in *Materials and Methods*. The media from each strain was immunoprecipitated with an antibody recognizing alpha factor-containing peptides. The positive control (Pos. control) comes from the secretion from a *kex2*Δ strain. In this SDS–PAGE system, a number of partially processed alpha factor peptides run with mature alpha factor at the dye front (arrowhead).

experiments were performed in strains lacking endogenous *VPS35* or *VPS26* but containing epitope (HA-) tagged yVps26 and myc-tagged hVps35 or hVps35R_{107}W. When normalized for equal levels of yVps26 (Figure 6C, upper panel), the immunoprecipitation of yVps26 (anti-HA) could coprecipitate a significant fraction of hVps35-myc but very little hVps35R_{107}W, while the supernatant (non-immunoprecipitated) portion of hVps35R_{107}W was increased (only 3.2% of the supernatant was loaded; Figure 6C, lower panel). The data strongly support that hVps35 requires R_{107} in order to engage Vps26 in a stable retromer interaction.

Effect of hVps35R_{107} on yeast retromer components

The increased turnover of hVps35-myc seemed consistent with the possibility that hVps35 might participate in unstable, defective yeast retromer protein complexes. To examine this more closely, strains were constructed bearing chromosomal, integrated copies of HA epitope-tagged Vps26, Vps29 and Vps17. HA-Vps5 was expressed under the control of its own promoter from a centromeric (CEN) plasmid in a *vps5*Δ strain. Triplicate independent yeast colonies bearing hVps35 exhibited levels of Vps29-HA or HA-Vps26 that were lower than their wild-type counterparts bearing vector alone (Figure 7). Interestingly, the R_{107}W mutation resulted in complete restoration of Vps29-HA and HA-Vps26 levels (Figure 7). Neither the levels of HA-Vps5 nor HA-Vps17 were affected by the presence of hVps35 (Figure 7). The data support that the expression and incorporation of hVps35 into defective yeast retromer induced instability of the two partner proteins in the large retromer subcomplex.

We also examined endogenous, untagged Vps26 in wild-type yeast cells expressing hVps35-myc. Western blotting clearly indicated that Vps26 protein levels were lower than in cells transformed with empty vector (Figure 8A, upper panel). However, the decrease in Vps26 levels was less

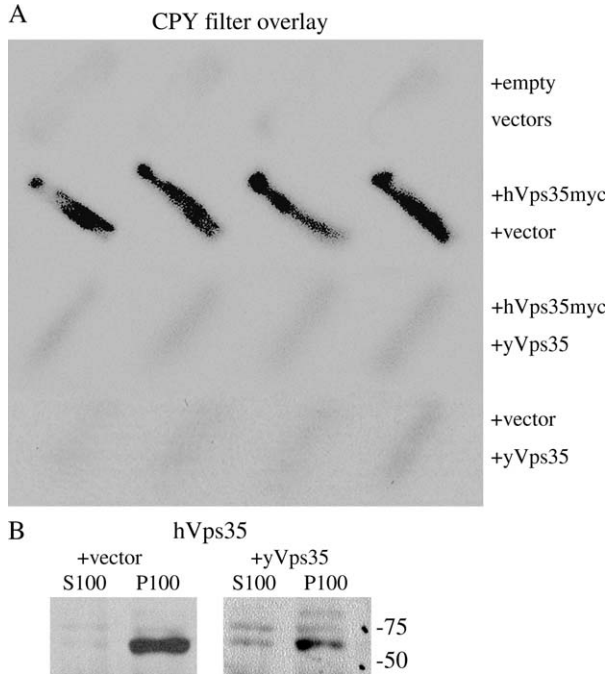

Figure 4: The dominant-negative phenotype induced by hVps35 is rescued by overexpression of yVps35. Panels A and B each employ yVps35 expressed from multicopy Yep plasmid driven by the *VPS35* promoter and hVps35myc from a YCp plasmid with expression driven by the *TDH3* promoter. A) The CPY filter overlay. Each wild-type strain is transformed with a centromeric plasmid listed first and a 2μ plasmid listed second with the protein (or lack of protein) encoded by these plasmids described (at right). B) Sedimentation behavior of hVps35-myc in the presence or absence of overexpressed yVps35. At left, hVps35 is nearly quantitatively associated with the pellet after centrifugation at 100 000 × ***g*** for 1 h (P100). At right, upon overexpression of yVps35, a fraction of hVps35 is displaced into the supernatant (S100). The hVps35 protein was identified by Western blotting with anti-myc.

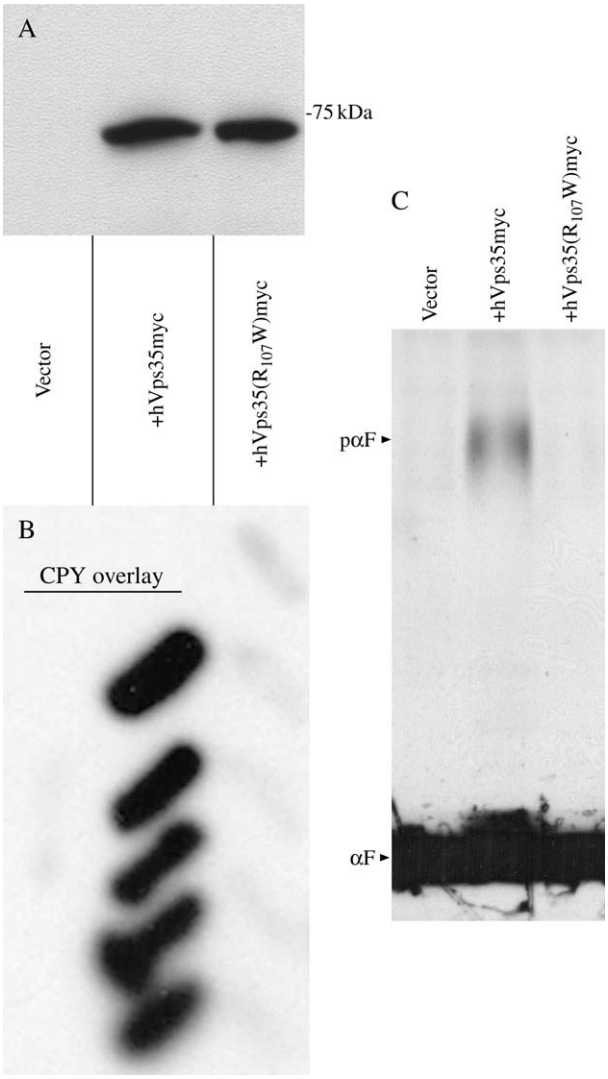

Figure 5: The dominant-negative phenotype induced by hVps35 is blocked by the $R_{107}W$ mutation. Panels A–C each employ constructs expressed from a YCp plasmid with expression driven by the *TDH3* promoter. A) Western blot establishing that the $R_{107}W$ mutant produces an expressed protein. B) Five independent transformants expressing the hVps35R_{107} mutant show loss of CPY secretion by filter blot compared with five transformants expressing hVps35. One colony of W303 cells transformed with empty vector (Vector) is shown as a negative control. C) Analysis of proalpha factor (pαF) processing by the strains shown in panels A and B was carried out as described in the legend to Figure 3. In this SDS–PAGE system, a number of partially processed alpha factor peptides run with mature alpha factor (αF) at the dye front.

apparent in *pre1 pre2* cells that are deficient for proteasomal degradation (Figure 8A, lower panel). Preservation of Vps26 levels by proteasome dysfunction did not rescue the *vps* (CPY missorting) phenotype caused by hVps35 (Figure 8B). The data suggest that sequentially, hVps35 first participates in formation of defective yeast retromer and thereafter, components of the dysfunctional complex are degraded at least in part by proteasomal activity. Thus, proteasomal blockade still does not prevent formation of a defective yeast retromer. By contrast, independent of proteasome function, introduction of the $R_{107}W$ mutation into hVps35 prevents the reduction of Vps26 levels (Figure 8A) while blocking the ability of hVps35 to produce a dominant-negative CPY secretion phenotype (Figure 8B).

Expression of hVps35R_{107}W in mammalian cells

In preliminary experiments (not shown), both HeLa cells and 293 cells were transiently transfected in which expression of hVps35 or hVps35R_{107}W was driven by a cytomegalovirus (CMV) promoter (likely to be stronger than the endogenous promoter for mammalian Vps35). The distribution of hVps35 showed smaller puncta in their cytoplasmic distribution than that seen for hVps35R_{107}W. We then examined transfected insulinoma cells to begin to explore the distribution of relevant markers in regulated secretory cells. As in HeLa and 293 cells, in transiently or

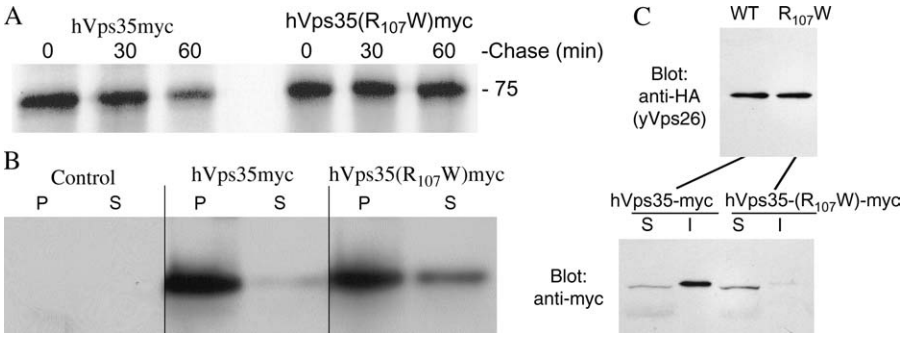

Figure 6: Turnover, sedimentation and Vps26 association of hVps35 with and without the $R_{107}W$ mutation. Panels A–C each employ constructs expressed from a YCp plasmid with expression driven by the *TDH3* promoter. A) Wild-type (W303) cells expressing hVps35-myc or hVps35R_{107}W-myc were metabolically labeled for 5 min with ^{35}S-amino acids and chased for the times indicated. At each chase time, cells were lysed and immunoprecipitated with anti-myc, normalized to trichloroacetic acid-precipitable counts. The immunoprecipitates were analyzed by SDS–PAGE and fluorography. B) Wild-type (W303) cells transformed to express the proteins shown or transformed with empty vector (Control) were lysed and the lysates were sedimented at 100 000 $\times$ ***g*** for 60 min as described in *Materials and Methods*. The pellet was resuspended in a volume identical to the supernatant volume, and equal volumes of the pellet and supernatant fractions were analyzed by SDS–PAGE and Western blotting with anti-myc. C) Yeast strain SNY217 carrying plasmid pVps26-HA (9) and either plasmid pGTH12 (hVps35-myc) or pGTH12-R_{107}W [hVps35(R_{107}W)-myc, also called simply R_{107}W] was lysed under native conditions. To confirm the presence of comparable starting amounts of yVps26-HA in each strain, 2% of each lysate was analyzed by SDS–PAGE and immunoblotting with mouse anti-HA antibody (upper gel). From the remaining lysates, immunoprecipitation was performed with rabbit anti-HA antibody using protein A–Sepharose. Fifty percent of the immunoprecipitate (I) and 3.2% of the supernatant (S) were analyzed by SDS–PAGE gel and immunoblotting with mouse anti-c-myc antibody (lower gel) to detect coprecipitated hVps35-myc and hVps35(R_{107}W)-myc. Densitometry of the bands, with correction for the percent loaded, back-calculated to the same total myc-tagged protein levels in each strain, and this was also directly confirmed by Western blotting (not shown). P, pellet; S, supernatant.

stably transfected INS-1 cells, hVps35-myc showed a more peripheral punctate cytoplasmic distribution than that of hVps35R_{107}W-myc (Figure 9). The expression and distribution of wild-type and mutant hVps35-myc in the stably transfected cells was then compared with that of CI-MPR (Figure 10). While hVps35R_{107}W-myc immunofluorescence was more enriched in the juxtanuclear region causing greater apparent antigen overlap in this region of the cell, overall MPR immunofluorescence intensity in such cells (Figure 10, arrow) appeared diminished. By quantification (in duplicate coverslips analyzed per each sample) using METAMORPH v 6.3r7 (Molecular Devices), cells expressing hVps35-myc exhibited on average 128 $\pm$ 27% MPR signal strength compared with cells expressing no exogenous mammalian Vps35, whereas cells expressing hVps35R_{107}W-myc exhibited only 26.5 $\pm$ 11% MPR signal strength. Finally, for insulin immunofluorescence, we turned to INS-832/13 cells, which maintain more insulin secretory granules than INS-1 cells. In cells transiently expressing hVps35-myc (Figure 11, upper row), a population of subplasmalemmal secretory granules was comparable to that in cells not expressing exogenous mammalian Vps35 (this phenotype was found in 91% of the cells). However, in cells expressing hVps35R_{107}W-myc, it was apparent that the expression coincided with the loss of most insulin secretory granules (Figure 11 arrows, lower row; this phenotype observed in 78.5% of the cells). These data suggest that hVps35R_{107}W has an altered intracellular membrane distribution and interferes with a number of post-Golgi trafficking functions.

Discussion

In this study, we have followed a general approach for developing selective dominant-interfering mutants of mammalian protein trafficking gene products by exploiting evolutionarily conserved protein interaction domains in conjunction with simple yeast genetics. Residue R_{98} of Vps35 appeared as an attractive initial candidate to explore mammalian Vps35 because (i) it is a common site of mutation amongst a collection of yeast mutants exhibiting dominant-negative behavior (17) and (ii) the site is highly conserved evolutionarily. Our companion manuscript suggests that yVps35-R_{98}W has diminished ability to bind its yVps26 partner and expression of the yVps35-R_{98}W mutant results in formation of defective retromer complexes (17). In the present study, replacement of the first 263 residues of yVps35 with the complementary residues of hVps35, despite imperfect *VPS35* function, also conveys enhanced dominant-negative behavior when the conserved Arg residue is mutated to Trp (Figure 1), strongly suggesting that the Arg residue – even when embedded within the hVps35 contextual sequence – engages a yeast retromer partner.

In contrast with yVps35, hVps35 exhibits dominant-negative behavior in yeast even before mutagenesis of the PRLYL motif (Figures 2 and 3). The sequences of hVps35 and yVps35 diverge substantially in the mid-molecule and in their carboxyl-terminal regions. Moreover, hVps35 and yVps35 are designed to sort different cargo

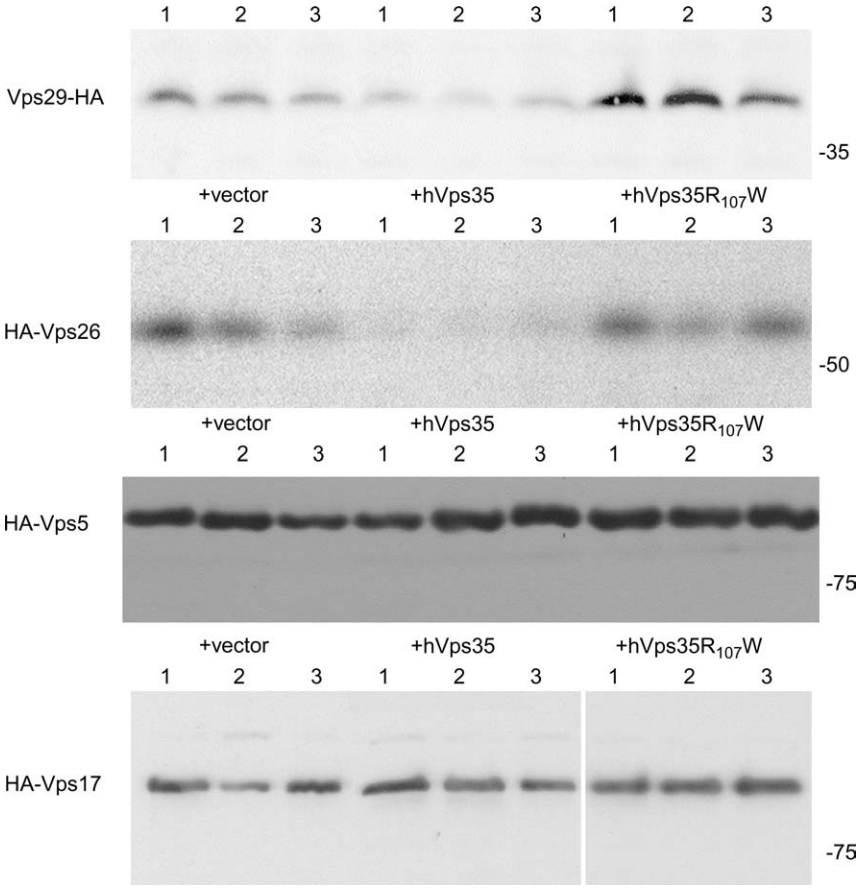

Figure 7: Immunoblotting to show steady-state levels of Vps29, Vps26, Vps5 and Vps17 in cells expressing hVps35, hVps35R$_{107}$W or empty vector (+vector). Constructs were expressed from a YCp plasmid with expression driven by the *TDH3* promoter. Each of the retromer components contains an HA-epitope tag as described in *Materials and Methods*. Triplicate independent transformants are shown. Note that only the components of the large retromer subcomplex (Vps29 and Vps26) exhibit reduced levels in the presence of hVps35. Quantification from these data shows that in cells expressing hVps35, there is at least a 60% reduction of Vps29 and a 75% reduction of Vps26 compared with the empty vector control. By contrast, cells expressing hVps35R$_{107}$W show no reduction in Vps29 or Vps26 levels.

molecules. Given these considerations, it does not seem surprising that hVps35-myc expression cannot complement a *vps35* null (Figure 2A) and would be more likely to associate with endogenous yeast components to form a dysfunctional retromer complex, specifically through its association with yVps26 (Figure 6C). The dominant-negative behavior is effectively reversed merely by raising yVps35 levels (Figure 4A), indicating that its specific perturbation occurs within the yeast retromer complex.

In this report, recruitment of hVps35-myc into dysfunctional retromer complexes is strongly suggested by its efficient coimmunoprecipitation with epitope-tagged yVps26 in a strain lacking *VPS35* and *VPS26*. However, when expressed as a dominant negative in (otherwise wild type) yeast, the expression of hVps35 evidently triggers degradation of endogenous Vps26 (and Vps29, see below). In this report, we demonstrate that dominant-negative phenotypes caused by hVps35 are totally blocked by the

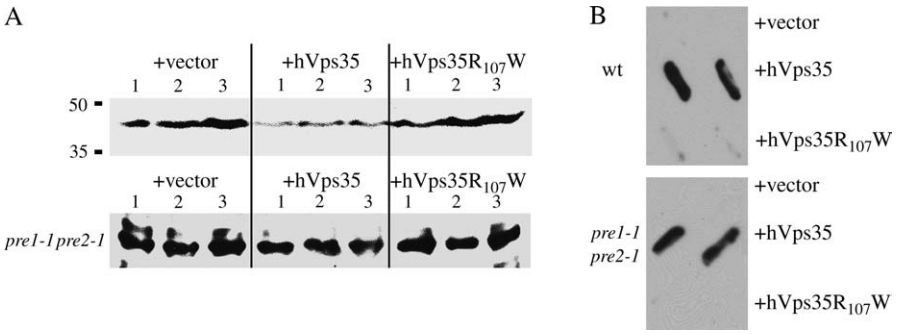

Figure 8: Expression of hVps35 in yeast induces proteasomal turnover of Vps26. Constructs were expressed from a YCp plasmid with expression driven by the *TDH3* promoter. A) Transformants (in triplicate) expressing hVps35, hVps35R$_{107}$W or empty vector (+vector). The *pre1-1 pre2-1* cells were grown, and all experiments were performed at 30°C. The Vps26 Western blot in the upper panel shows the results from control cells, while the lower panel (*pre1-1 pre2-1*) shows the results from proteasome-deficient cells. B) The CPY filter overlay from the strains shown in panel A. wt, wild type.

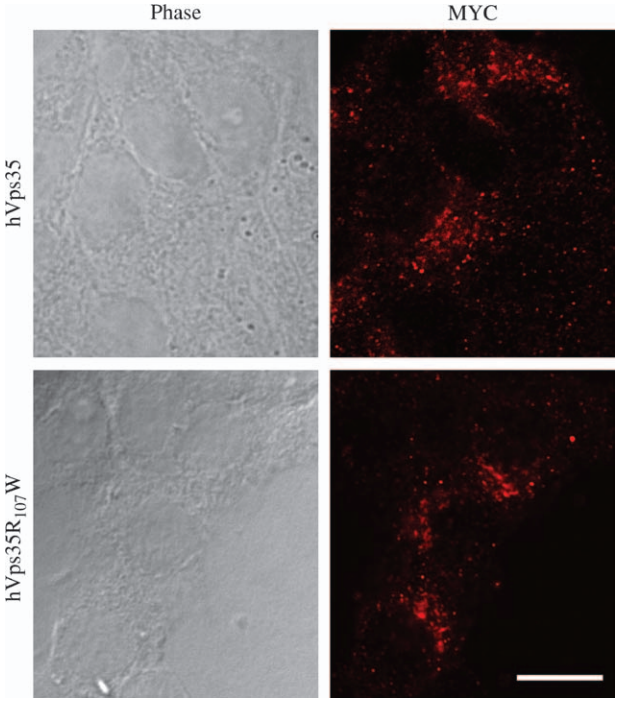

Figure 9: Expression of myc-tagged hVps35 or hVps35R$_{107}$W in INS-1 cells. By Western blotting (not shown), INS-1 cells stably expressing hVps35 have equal protein levels to those of the cells expressing hVps35R$_{107}$W. Cells expressing hVps35 show anti-myc labeling in small vesicles throughout the cytoplasm, whereas the R$_{107}$W mutant is concentrated in juxtanuclear structures. Scale bar = 10 μm.

introduction of the R$_{107}$W mutation – including both CPY secretion and proalpha factor processing (Figure 5B,C). Loss of the dominant negative occurs despite that a pool of hVps35R$_{107}$W can still be pelleted at 100 000 × ***g*** for 1 h (Figure 6B). We do not know precisely what this persistent sedimentation signifies, but we note that this behavior is virtually identical to the degree of displacement of hVps35-myc from membranes when its specific binding sites are competed away by overexpression of yVps35 (Figure 4B); thus, we interpret the remaining as 'non-specific sedimentation' that may occur even when hVps35 and hVps35R$_{107}$W (both driven by the strong constitutive *TDH3* promoter) are expressed in excess of the stoichiometry of their yVps26 retromer partner. Indeed, we have found that both hVps35 and hVps35R$_{107}$W still sediment in strains lacking *VPS26* (not shown), and a similar observation has been made for yVps35 in strains lacking *VPS29* (18). Potentially, this additional sedimentation (which requires significant centrifugal force – somewhere between 62 000 and 82 000 × ***g***; data not shown) might occur through direct membrane association of hVps35 or hVps35R$_{107}$W, perhaps including phospholipid interactions.

We find that hVps35 has a slightly faster turnover in yeast cells than hVps35R$_{107}$W (Figure 6A), but more important is the reduced level of yVps26 and yVps29 (Figure 7). This reduction is at least partially dependent upon proteasome activity, supporting that hVps35 participates in an unstable complex resulting in the proteasomal destruction of these dynamically associating subunits (Figure 8). Importantly, proteasomal dysfunction does not restore normal retromer

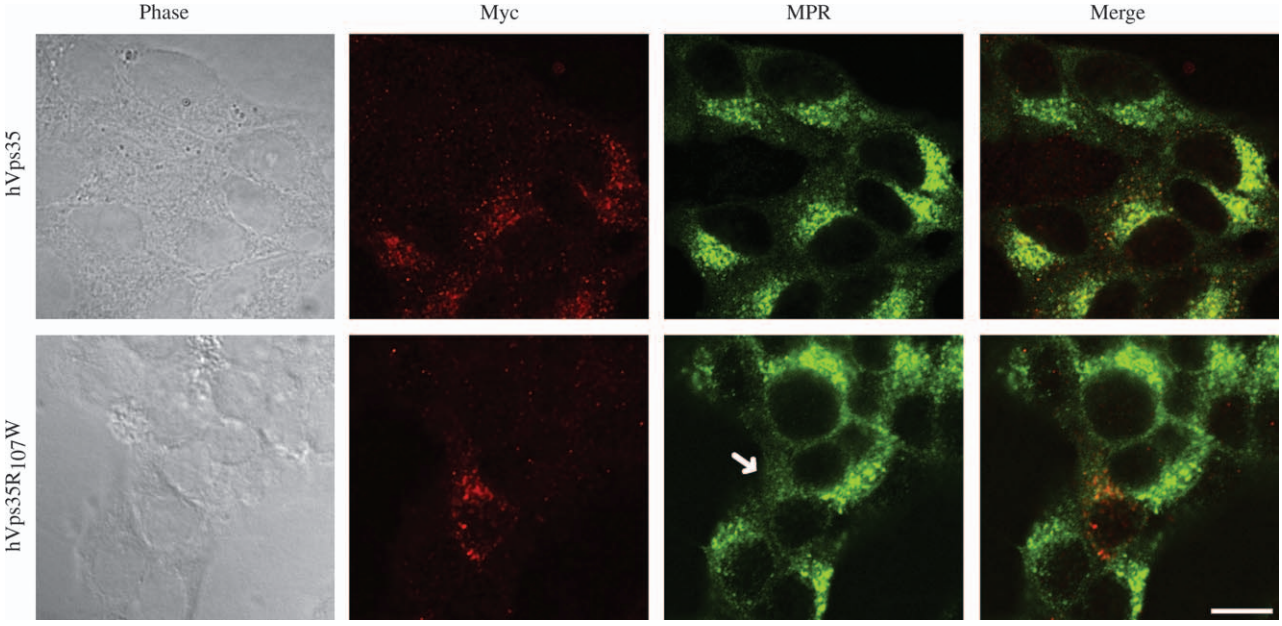

Figure 10: Double immunofluorescence labeling of myc-tagged hVps35 or hVps35R$_{107}$W with the CI-MPR (MPR) in INS-1 cells. The hVps35R$_{107}$W mutant tends to concentrate in juxtanuclear structures, and MPR exhibits decreased overall immunofluorescence intensity in these cells compared with cells that do not express hVps35R$_{107}$W (see text). Scale bar = 10 μm. The arrow highlights decreased MPR immunofluorescence intensity in cells expressing the mutant hVps35.

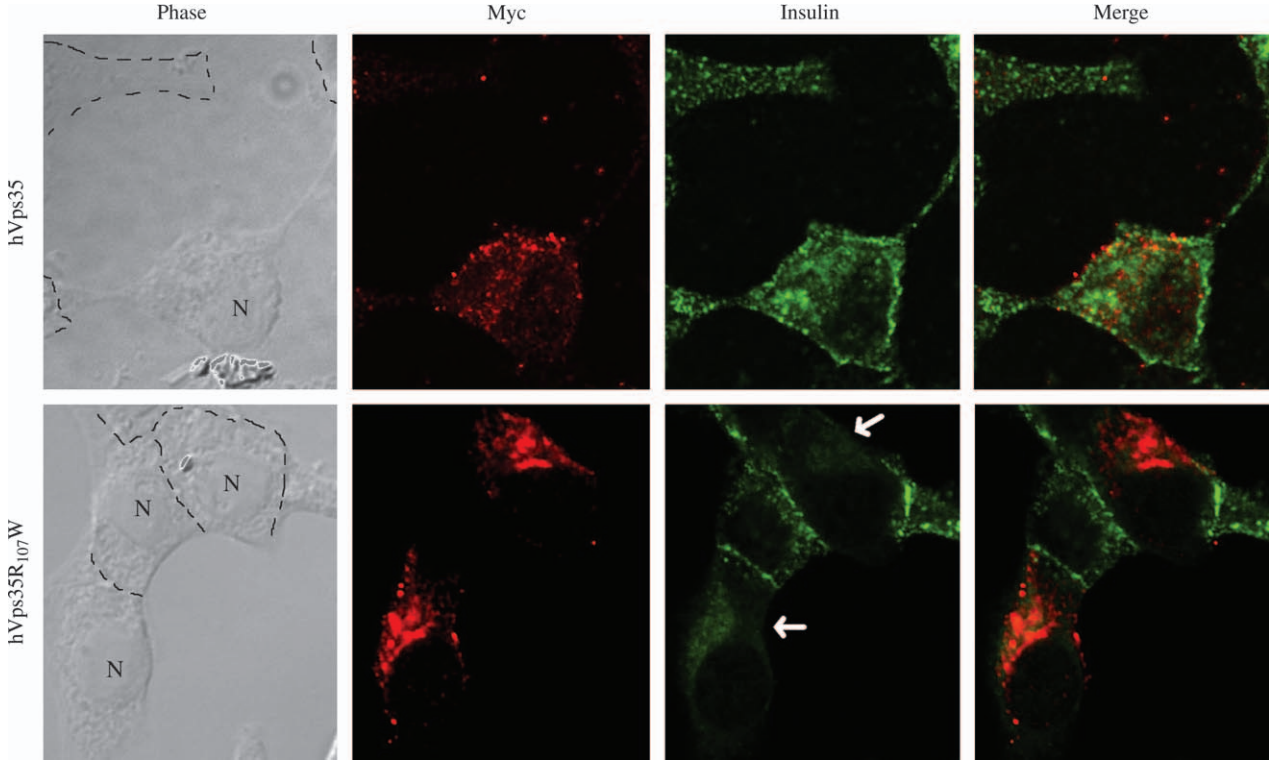

Figure 11: Double immunofluorescence labeling of myc-tagged hVps35 or hVps35R_{107}W with anti-insulin in INS-832/13 cells. Transient expression of hVps35 (upper panels) does not impair accumulation of subplasmalemmal insulin secretory granules. By contrast, expression of the R_{107}W mutant in these cells inhibits granule accumulation (lower panels and see text). Dashed lines drawn on phase-contrast images outline the cell borders. 'N' highlights selected nuclei. Scale bar = 10 μm. The arrows highlight decreased immunofluorescent insulin secretory granules in cells expressing the mutant hVps35.

activity, proving that the hVps35 protein cannot function with yeast retromer partners (Figure 2A) even when protected from degradation (Figure 8B). Taken together, these data signify that retromer subunits that assemble into defective complexes are destroyed, and this may be one mechanism to maintain proper intracellular stoichiometry of functional retromer-binding partners in cells. In support of this conclusion, selective knockdown of either mammalian Vps35 or Vps26 expression has been found to be associated with concomitant knockdown of other members of the Vps35/26/29 subcomplex (8,14,19), and similar instability has previously been reported also in yeast cells (5,9).

In mammalian cells, hVps35R_{107}W has a more concentrated juxtanuclear distribution than does hVps35 (Figures 9–11). Expression of hVps35R_{107}W exhibits some overlap of distribution with MPRs in the juxtanuclear region but also causes a decrease in MPR signal strength (e.g. Figure 10), which has often been reported as a consequence of perturbed MPR trafficking. Further, the population insulin granules of the regulated secretory pathway are adversely affected by expression of hVps35R_{107}W (Figure 11). While these studies are consistent with the previous work suggesting a role for retromer in MPR trafficking in mammalian cells (8), they also imply potential significance of retromer function in the recycling of secretory granule membrane proteins, which is an area that remains largely unexplored (20–22).

In conclusion, we have established that the conserved PRLYL motif of hVps35 interacts with yVps26, affecting function of the yeast retromer. Work is ongoing to further characterize the significance of dominant-negative hVps35R_{107}W in mammalian cells.

Materials and Methods

Yeast strains and media

Standard yeast media and genetic manipulations were as described previously (23). Unless otherwise indicated (Table 1), strains employed in this study are isogenic to W303 or SNY36-9A (24). Strain *vps35::LEU2* is the *eis1* mutant of L5145/pMI316, displaying *e*nhanced immunoreactive *i*nsulin *s*ecretion after random mutagenesis and screening (1). Yeast strain SNY183 was prepared from the strain LSY2 by insertional replacement of *VPS29* with a *VPS29*::3xHA-KanR allele using the method of Longtine et al. (25). Similarly, the SNY175 and SNY176 strains were prepared from strain LSY2 (26) by insertion of a 3xHA tag at the 3′ end of the *VPS17* and *VPS26* open reading frames (ORFs) using a polymerase chain reaction (PCR)-mediated approach (27).

Plasmids and molecular biology

pRSGLC is a *TRP1*-marked centromeric plasmid [pRS314 (28)] bearing the *TDH3* promoter (29). For detection of Vps5, cells were transformed with

Table 1: Yeast strains used in this study

Strains	Genotype	Source
SNY36-9A	*MATa leu2-3,112 ura3-52 his3-Δ200 trp1-901 suc2-9 pho8Δ::ADE2*	(24)
LSY2	*MATa leu2-3,112 ura3-52 his3-Δ200 trp1-901 suc2-9 pho8Δ::ADE2 pep4Δ::TRP1*	(33)
SNY175	*MATa leu2-3,112 ura3-52 his3-Δ200 trp1-901 suc2-9 pho8Δ::ADE2 pep4Δ::TRP1 VPS17::3xHA*	This study
SNY176	*MATa leu2-3,112 ura3-52 his3-Δ200 trp1-901 suc2-9 pho8Δ::ADE2 pep4Δ::TRP1 VPS26::3xHA*	This study
SNY183	*MATa leu2-3,112 ura3-52 his3-Δ200 trp1-901 suc2-9 pho8Δ::ADE2 pep4Δ::TRP1 VPS29::3xHA*	This study
PBY35	*MATa leu2-3,112 ura3-52 his3-Δ200 trp1-901 suc2-9 pho8Δ::ADE2 pep4Δ::TRP1 vps5Δ::HIS3 etc.*	(17)
W303	*MATa ade2-1 can1-100 his3-11 leu2-3,112 trp1-1 ura3-52*	(34)
vps35Δ	*MATα ade2-1 can1-100 his3-11 leu2-3,112 trp1-1 ura3-52 vps35Δ::HIS3*	This study
KY146	*MATa his3-11 leu2-3,112 ura3-52 can1-100*	(35)
KY148	*MATa his3-11 leu2-3,112 ura3-52 can1-100 pre1-1 pre2-1*	(35)
BFY106-4D	*MATa ade2-1 can1-100 his3-11,15 leu2-3,112 trp1-1 ura3-1 kex2Δ::HIS3-A*	(36)
SNY217	*MATa leu2-3,112 ura3-52 his3-Δ200 trp1-901 suc2-8 pho8Δ::ADE2 pep4Δ−ΔH3 vps35Δ::HIS3 vps26Δ::NatR*	This study

pAH31, a URA3-marked centromeric plasmid encoding 1xHA-yVps5 (30). In this epitope-tagged construct, the 6th residue of yVps5 was mutated from Asn to Leu. pAH60 is a URA3-marked 2μ plasmid (pYEp352) carrying an approximately 3.9-kb *Eco*RI–*Sac*I DNA fragment containing *yVPS35*. pAH60-hpX is a series of dominant-negative mutants obtained from PCR mutagenesis on pAH60. pRS314-hpA is a TRP1-marked centromeric plasmid carrying the same approximately 3.9-kb *yVPS35* fragment as pAH60. pRS314-hpX are the corresponding dominant-negative *vps35* alleles from the pAH60-hpX series subcloned into the pRS314 backbone. The hVps35-myc complementary DNA (cDNA) was kindly provided Dr C. Renfrew Haft (National Institute of Diabetes, Digestive Diseases and Kidney, National Institutes of Health, Bethesda, MD, USA). pT35 encodes hVps35-myc subcloned directly after the *TDH3* promoter using *Bam*HI and *Sal*I sites of pRSGLC. pT35RW is the pT35 plasmid encoding hVps35 with the $R_{107}W$ single point mutation. pGTH11 encodes the N-terminal HA-tagged hVps35, subcloned directly after the *TDH3* promoter, into the *Bam*HI/*Sal*I of pRSGLC; in the coding sequence, the first five residues of hVps35 were replaced by 16 residues containing an initiator methionine and the HA epitope tag. pcDNA3–hVps35 (or pcDNA3–hVps35RW) encodes the C-terminal myc-tagged hVps35 (or $hVps35R_{107}W$ mutant) subcloned directly downstream of the *CMV* promoter using the *Bam*HI/*Xho*I sites of vector pcDNA3 (Invitrogen). To make the human–yeast hybrid *VPS35* construct known as pNHCY1 an approximately 800 DNA fragment from pGTH11 was amplified by the following primers: GACGTCCATGAGATATT-CTTGAGC (that introduces an *Aat*II site, underlined) and CACCAAGAACTTAG (sequence from *TDH3* promoter). The PCR product that includes part of the *TDH3* promoter sequence, a *Bam*HI site, ATG, encoded HA-tag sequence (48 nucleotides) and an N-terminal fragment of hVps35 up to residue 263, as well as the *Aat*II site, was subcloned into the pGEM T-vector and linked to an *Aat*II–*Sal*I fragment from *yVPS35* (encoding the complete C-terminal fragment of yVps35 beginning at residue 245). The hybrid version was then subcloned to pRSGLC directly downstream of the *TDH3* promoter to make plasmid pNHCY1. Plasmid pNHCY1-RW is the mutant derivative of pNHCY1.

Materials

Rabbit polyclonal anti-myc from Santa Cruz Biotech, Inc. was used for immunoblotting at a 1:4000 dilution. Guinea-pig anti-insulin was from Linco Research. Mouse monoclonal antibody (mAb) anti-myc (9E10) was produced in the University of Michigan Hybridoma Core Lab and purchased at Santa Cruz Biotech, Inc. Rabbit polyclonal and mouse monoclonal anti-HA were from Covance Research Co.. Mouse mAb anti-CPY was from Molecular Probes. Rabbit polyclonal anti-alpha factor antibody (RW1) was the kind gift of Dr D. Shields (Albert Einstein College of Medicine, Bronx, NY, USA). Rabbit polyclonal anti MPR was the kind gift of Dr L. Matovcik (Yale University School of Medicine, New Haven, CT, USA). Rabbit polyclonal anti-yVps26 was the kind gift of Dr M. Seaman (University of Cambridge, UK). Secondary antibodies and peroxidase conjugates were from Jackson Immunolaboratories; Zysorbin was from Zymed; protein A and protein G agarose were from Sigma. ^{35}S-cysteine and ^{35}S-methionine/cysteine mixture (Expre^{35}S^{35}S) were purchased from New England Nuclear. For immunoblotting, bands were visualized by enhanced chemiluminescence (Amersham).

CPY filter-blot assay

To assay secretion of CPY, cell patches were replica plated onto nitrocellulose filters placed on top of the plates. After 24 h, the filter was washed and processed for immunoblotting with mouse mAb anti-CPY and a peroxidase-conjugated secondary antibody (1:10 000 dilution).

Proalpha factor secretion

To examine secretion of proalpha factor, cells were grown to mid-log phase in synthetic complete medium without methionine and cysteine. Cells were harvested and resuspended at 0.8 optical density (OD_{600})/mL in fresh medium with 1 mg/mL bovine serum albumin. Five hundred microCurie of ^{35}S-amino acid mixture was added to each sample and incubation was continued for 50 min at room temperature with shaking. Media were separated from cells by centrifugation at 19 500 × ***g*** for 5 min. sodium dodecyl sulfate (SDS) was added to the medium to a final concentration of 1%, and samples were boiled for 3 min. Secretion of alpha factor-containing peptides was recovered by immunoprecipitation with the RW1 rabbit polyclonal anti-alpha factor antibody and analyzed by SDS–15%–PAGE and fluorography.

Western blot and membrane sedimentation assay

Steady-state levels of myc or HA-tagged proteins (or endogenous yVps26p) were analyzed in cell lysates prepared from mid-log cultures by vortexing with glass beads as described previously (31). Unlysed cells were removed by centrifugation at 4500 × ***g*** × min twice at 4°C. Sample loading was normalized to lysate protein as measured by bicinchoninic acid protein assay (Pierce Biotech, Inc.). After SDS–PAGE and electrotransfer to nitrocellulose, blots were probed with anti-myc, anti-HA or anti-Vps26 (1:250 dilution) and a peroxidase-conjugated secondary antibody (1:5000 dilution). Bands were visualized by enhanced chemiluminescence (Amersham).

Membrane sedimentation assays were carried out after harvesting cell lysates using the same lysis method (31). Unlysed cells were removed by centrifugation at 4500 × ***g*** × min twice at 4°C. The 4500 × ***g***-min supernatant was then diluted to 1 μg/μL. Three hundred micrograms of cell lysates were centrifuged at 100 000 × ***g*** for 60 min to generate pellet (P100) and supernatant (S100) fractions. The P100 pellet was resuspended in 300-μL lysis buffer (31) to match the volume of the supernatant. All steps, performed at 4°C, included presence of a protease inhibitor cocktail (aprotinin 0.25 ug/mL, leupeptin 0.1 mM, pepstatin 10 uM, ethylenediaminetetraacetic acid (EDTA) 5 mM and E64 10 uM). The supernatant and pellet protein distribution was measured by SDS–PAGE and Western blotting.

Metabolic labeling and immunoprecipitation of CPY or hVps35-myc

Cells were grown to exponential phase in synthetic complete medium without methionine and cysteine and then sedimented at 3000 × ***g*** for

5 min and resuspended at 1 OD_{600}/mL in the same medium. Cells were labeled with Expre^{35}S^{35}S at 0.1 mCi per 1 OD_{600} cells for 5 min at room temperature and chased in the presence of 10 mM unlabeled methionine and cysteine. At various chase times, aliquots were placed on ice in the presence of 10 mM NaN_3. In preparation for immunoprecipitation of CPY or hVps35-myc, cells were then sedimented at 3000 × ***g*** for 5 min; in addition, the supernatant containing secreted proteins was collected for further analysis. Lysates were prepared and resuspended in RIPA buffer (10 mM Tris, pH 7.5, 150 nM NaCl, 2 mM EDTA, 1% Nonidet P-40, 1% deoxycholate and 0.1% SDS). All samples received a protease inhibitor cocktail (aprotinin 0.25 μg/mL, leupeptin 0.1 mM, pepstatin 10 μM, EDTA 5 mM and E64 10 μM). Samples were precleared with 20 μL Zysorbin for 30 min (Zymed) and then immunoprecipitated either with 1 μL mouse mAb anti-CPY and protein G–Sepharose beads or with 1 μL rabbit anti-myc antibody and protein A–Sepharose beads.

Mammalian cell culture, transfection and immunofluorescence

INS-1 and INS-832/13 cells were cultured as described previously (32). A cDNA encoding wild-type hVps35-myc or hVps35-mycR_{107}W was subcloned into the pcDNA3 (CMV promoter-driven) expression vector (Invitrogen). Plasmid DNA was transfected into cells using lipofectamine (Gibco/Brl). Transfected INS-1 cells were selected with G418 and then grown on glass coverslips and prepared for immunofluorescence. To allow proinsulin egress from the endoplasmic reticulum, processing and insulin accumulation in secretory granules, cells were treated with cycloheximide (10 μg/mL) for 60 min before fixation. Cells were then fixed with 4% formaldehyde and permeabilized with 0.1% Triton-X-100. After fixation, the cells were incubated for 30 min in 5% newborn bovine serum in PBS containing 0.02% NaN_3 (wash) and then processed for immunodetection. Primary antibodies were diluted in wash, mouse mAb anti-Myc at 1:250 (or rabbit polyclonal anti-Myc at 1:500) together with anti-insulin or anti-MPR antibodies (each used at 1:500); antibodies were incubated with the cells for 30 min at room temperature. To assess background staining, anti-myc antibodies were incubated with untransfected cells, whereas guinea-pig IgGs served as a negative control for the insulin antibody. Bound antibodies were detected with secondary antibodies that were Alexa Fluor 488 tagged (Molecular Probes), Alexa Fluor 555 tagged (Molecular Probes) or amino methylcoumarin-tagged (Jackson ImmunoResearch). Fluorescence was monitored with an Olympus FV500 confocal laser-scanning microscope (Olympus America Inc.) using standard filter settings and sequential scanning to avoid overlap of emission from the fluorophores. The thickness of the optical sections was set to 0.486 mm. Where comparisons between samples were employed, digital images were captured at fixed exposure settings and Photoshop files were transferred with identical settings for image presentation.

Acknowledgments

This work was supported by grants from the National Institutes of Health (NIH): DK48280 to P. A. and GM053449 to S. F. N. We acknowledge the assistance of the Morphology and Image Analysis Core, the Hybridoma Core and the Molecular Biology Core of the Michigan Diabetes Research and Training Center, funded by NIH5P60 DK20572. We thank the members of the lab of A. Chang (University of Michigan) for their helpful discussions and assistance.

References

1. Zhang B-y, Chang A, Kjeldsen TB, Arvan P. Intracellular retention of newly-synthesized insulin in yeast is caused by endoproteolytic processing in the Golgi complex. J Cell Biol 2001;153:1187–1197.
2. Seaman MN. Recycle your receptors with retromer. Trends Cell Biol 2005;15:68–75.
3. Hettema EH, Lewis MJ, Black MW, Pelham HR. Retromer and the sorting nexins Snx4/41/42 mediate distinct retrieval pathways from yeast endosomes. EMBO J 2003;22:548–557.
4. Griffin CT, Trejo J, Magnuson T. Genetic evidence for a mammalian retromer complex containing sorting nexins 1 and 2. Proc Natl Acad Sci U S A 2005;102:15173–15177.
5. Seaman MN, McCaffery JM, Emr SD. A membrane coat complex essential for endosome-to-Golgi retrograde transport in yeast. J Cell Biol 1998;142:665–681.
6. Seaman MN, Williams HP. Identification of the functional domains of yeast sorting nexins Vps5p and Vps17p. Mol Biol Cell 2002;13:2826–2840.
7. Nothwehr SF, Ha SA, Bruinsma P. Sorting of yeast membrane proteins into an endosome-to-Golgi pathway involves direct interaction of their cytosolic domains with Vps35p. J Cell Biol 2000;151:297–310.
8. Arighi CN, Hartnell LM, Aguilar RC, Haft CR, Bonifacino JS. Role of the mammalian retromer in sorting of the cation-independent mannose 6-phosphate receptor. J Cell Biol 2004;165:123–133.
9. Reddy JV, Seaman MN. Vps26p, a component of retromer, directs the interactions of Vps35p in endosome-to-Golgi retrieval. Mol Biol Cell 2001;12:3242–3256.
10. Coudreuse DY, Roel G, Betist MC, Destree O, Korswagen HC. Wnt gradient formation requires retromer function in Wnt-producing cells. Science 2006;312:921–924.
11. Prasad BC, Clark SG. Wnt signaling establishes anteroposterior neuronal polarity and requires retromer in C. elegans. Development 2006;133:1757–1766.
12. Edgar AJ, Polak JM. Human homologues of yeast vacuolar protein sorting 29 and 35. Biochem Biophys Res Commun 2000;277:622–630.
13. Oliviusson P, Heinzerling O, Hillmer S, Hinz G, Tse YC, Jiang L, Robinsona DG. Plant retromer, localized to the prevacuolar compartment and microvesicles in Arabidopsis, may interact with vacuolar sorting receptors. Plant Cell 2006;18:1239–1252.
14. Seaman MN. Cargo-selective endosomal sorting for retrieval to the Golgi requires retromer. J Cell Biol 2004;165:111–122.
15. Haft CR, de la Luz Sierra M, Bafford R, Lesniak MA, Barr VA, Taylor SI. Human orthologs of yeast vacuolar protein sorting proteins Vps26, 29, and 35: assembly into multimeric complexes. Mol Biol Cell 2000;11:4105–4116.
16. Collins BM, Skinner CF, Watson PJ, Seaman MN, Owen DJ. Vps29 has a phosphoesterase fold that acts as a protein interaction scaffold for retromer assembly. Nat Struct Mol Biol 2005;12:594–602.
17. Restrepo R, Zhao X, Peter H, Zhang B-y, Arvan P, Nothwehr SF. Structural features of Vps35p involved in interaction with other subunits of the retromer complex. Traffic 2007; doi: 10.1111/j.1600-0854.2007.00659.x.
18. Seaman MN, Marcusson EG, Cereghino JL, Emr SD. Endosome to Golgi retrieval of the vacuolar protein sorting receptor, Vps10p, requires the function of the VPS29, VPS30, and VPS35 gene products. J Cell Biol 1997;137:79–92.
19. Verges M, Luton F, Gruber C, Tiemann F, Reinders LG, Huang L, Burlingame AL, Haft CR, Mostov KE. The mammalian retromer regulates transcytosis of the polymeric immunoglobulin receptor. Nat Cell Biol 2004;6:763–769.
20. Ferraro F, Eipper BA, Mains RE. Retrieval and reuse of pituitary secretory granule proteins. J Biol Chem 2005;280:25424–25441.
21. Milgram SL, Mains RE, Eipper BA. Identification of routing determinants in the cytosolic domain of a secretory granule-associated integral membrane protein. J Biol Chem 1996;271:17526–17535.

22. Wasmeier C, Hutton JC. Molecular cloning of phogrin, a protein-tyrosine phosphatase homologue localized to insulin secretory granule membranes. J Biol Chem 1996;271:18161–18170.
23. Sherman F, Hicks JB, Fink GR. Methods in Yeast Genetics: A Laboratory Manual. Cold Spring Harbor, NY: Cold Spring Harbor Laboratory Press; 1986.
24. Nothwehr SF, Conibear E, Stevens TH. Golgi and vacuolar membrane proteins reach the vacuole in vps1 mutant yeast cells via the plasma membrane. J Cell Biol 1995;129:35–46.
25. Longtine MS, McKenzie A, Demarini DJ, Shah NG, Wach A, Brachat A, Philippsen P, Pringle JR. Additional modules for versatile and economical PCR-based gene deletion and modification in Saccharomyces cerevisiae. Yeast 1998;14:953–961.
26. Spelbrink RG, Nothwehr SF. The yeast GRD20 gene is required for protein sorting in the trans-Golgi network/endosomal system and for polarization of the actin cytoskeleton. Mol Biol Cell 1999;10:4263–4281.
27. Schneider BL, Seufert W, Steiner B, Yang QH, Futcher AB. Use of polymerase chain reaction epitope tagging for protein tagging in Saccharomyces cerevisiae. Yeast 1995;11:1265–1274.
28. Sikorski RS, Hieter P. A system of shuttle vectors and yeast host strains designed for efficient manipulation of DNA in Saccharomyces cerevisiae. Genetics 1989;122:19–27.
29. Warner JR. Labeling of RNA and phosphoproteins in Saccharomyces cerevisiae. Methods Enzymol 1991;194:423–428.
30. Nothwehr SF, Hindes AE. The yeast VPS5/GRD2 gene encodes a sorting nexin-1-like protein required for localizing membrane proteins to the late Golgi. J Cell Sci 1997;110:1063–1072.
31. Chang A, Slayman CW. Maturation of the yeast plasma membrane [H+]ATPase involves phosphorylation during intracellular transport. J Cell Biol 1991;115:289–295.
32. Asfari M, Janjic D, Meda P, Li G, Halban PA, Wollheim CB. Establishment of 2-mercaptoethanol-dependent differentiated insulin-secreting cell lines. Endocrinology 1992;130:167–178.
33. Johnston HD, Foote C, Santeford A, Nothwehr SF. Golgi-to-late endosome trafficking of the yeast pheromone processing enzyme Ste13p is regulated by a phosphorylation site in its cytosolic domain. Mol Biol Cell 2005;16:1456–1468.
34. Thomas BJ, Rothstein R. Elevated recombination rates in transcriptionally active DNA. Cell 1989;56:619–630.
35. Kornitzer D, Raboy B, Kulka RG, Fink GR. Regulated degradation of the transcription factor Gcn4. EMBO J 1994;13:6021–6030.
36. Luo W, Chang A. Novel genes involved in endosomal traffic in yeast revealed by suppression of a targeting-defective plasma membrane ATPase mutant. J Cell Biol 1997;138:731–746.